

Обзор ArXiv/astro-ph,  
18-22 мая 2020 года

От Сильченко О.К.

# ArXiv: 2005.09661, Nature

## **A Cold, Massive, Rotating Disk 1.5 Billion Years after the Big Bang**

Marcel Neeleman<sup>1</sup>, J. Xavier Prochaska<sup>2,3</sup>, Nissim Kanekar<sup>4</sup> & Marc Rafelski<sup>5,6</sup>

<sup>1</sup>*Max-Planck-Institut für Astronomie, Königstuhl 17, D-69117, Heidelberg, Germany*

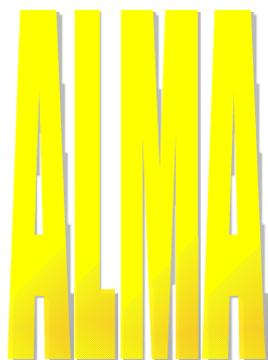
<sup>2</sup>*Department of Astronomy & Astrophysics, UCO/Lick Observatory, University of California, 1156 High Street, Santa Cruz, CA 95064, USA*

<sup>3</sup>*Kavli Institute for the Physics and Mathematics of the Universe (Kavli IPMU), The University of Tokyo, 5-1-5 Kashiwanoha, Kashiwa, 277-8583, Japan*

<sup>4</sup>*National Centre for Radio Astrophysics, Tata Institute of Fundamental Research, Pune University, Pune 411007, India*

<sup>5</sup>*Space Telescope Science Institute, Baltimore, MD 21218, USA*

# Доп. Наблюдения выборки 6 DLA – ЭТОТ САМЫЙ ЯРКИЙ



**HST**

**JVLA**

[C II] right ascension, R. A. <sub>[C II]</sub>	(J2000)	08:17:40.8676(18)
[C II] declination, Decl. <sub>[C II]</sub>	(J2000)	+13:51:38.219(19)
[C II] flux density size, $A_{[C II]}$	("×")	$(0.63 \pm 0.07 \times 0.43 \pm 0.05)$
[C II] position angle, P. A. <sub>[C II]</sub>	(°)	$109 \pm 13$
[C II] redshift, $z_{[C II]}$		$4.2603 \pm 0.004$
Peak [C II] flux, $S_{[C II],peak}$	(mJy)	$16.8 \pm 1.3$
[C II] line width, $FWHM_{[C II]}$	(km s <sup>-1</sup> )	$400 \pm 40$
Integrated [C II] flux, $\int S_{[C II]} dv$	(Jy km s <sup>-1</sup> )	$(5.8 \pm 0.4)$
[C II] luminosity, $L_{[C II]}$	( $L_{\odot}$ )	$(3.26 \pm 0.22) \times 10^9$
Continuum right ascension, R.A. <sub>cont</sub>	(J2000)	08:17:40.8655(12)
Continuum declination, Decl. <sub>cont</sub>	(J2000)	+13:51:38.223(10)
Continuum size, $A_{cont}$	("×")	$(0.41 \pm 0.05 \times 0.24 \pm 0.03)$
Continuum position angle, P.A. <sub>cont</sub>	(°)	$98 \pm 11$
Continuum flux, $S_{cont}$	(mJy)	$1.28 \pm 0.15$
Total infrared luminosity, $L_{TIR}$	( $L_{\odot}$ )	$1.2^{+2.3}_{-0.7} \times 10^{12}$
1.6 μm right ascension, R.A. <sub>1.6μm</sub>	(J2000)	08:17:40.852(12)
1.6 μm declination, Decl. <sub>1.6μm</sub>	(J2000)	+13:51:38.19(9)
1.6 μm size, $A_{1.6μm}$	("×")	$(1.2 \pm 0.5 \times 0.26 \pm 0.14)$
1.6 μm position angle, P.A. <sub>1.6μm</sub>	(°)	$114 \pm 8$
1.6 μm AB magnitude, $M_{AB}$		$25.1 \pm 0.2$
CO(2–1) right ascension, R.A. <sub>CO</sub>	(J2000)	08:17:40.53
CO(2–1) declination, Decl. <sub>CO</sub>	(J2000)	+13:51:34.6
CO(2–1) redshift, $z_{CO}$		$4.2589 \pm 0.0010$
Integrated CO(2–1) flux, $\int S_{CO} dv$	(Jy km s <sup>-1</sup> )	$0.14 \pm 0.04$
CO(2–1) luminosity, $L_{CO}$	( $L_{\odot}$ )	$(9.6 \pm 2.8) \times 10^6$
CO(2–1) luminosity, $L'_{CO}$	(K km s <sup>-1</sup> pc <sup>2</sup> )	$(2.4 \pm 0.7) \times 10^{10}$

# Во всех наблюдениях его увидели

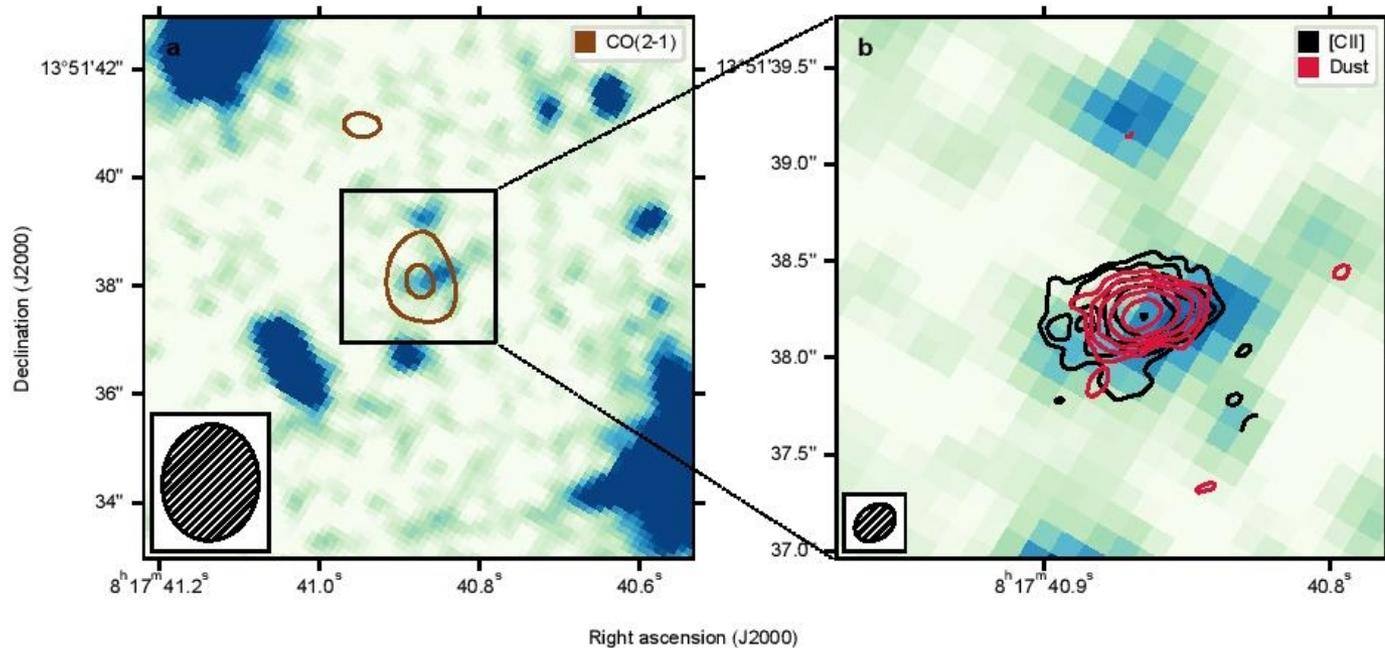


**Fig. 4.** HST imaging of DLA0817g with CO, [C II] and dust continuum contours. The F160W filter on HST's Wide Field Camera 3 was used to probe the rest-frame near-UV emission of the galaxy. **a**, The field surrounding DLA0817g. The bright source in the bottom right corner is the quasar whose sightline contains the  $z = 4.26$  absorber. Overlaid on this figure in contours is the

# Поле скоростей прохладного газа

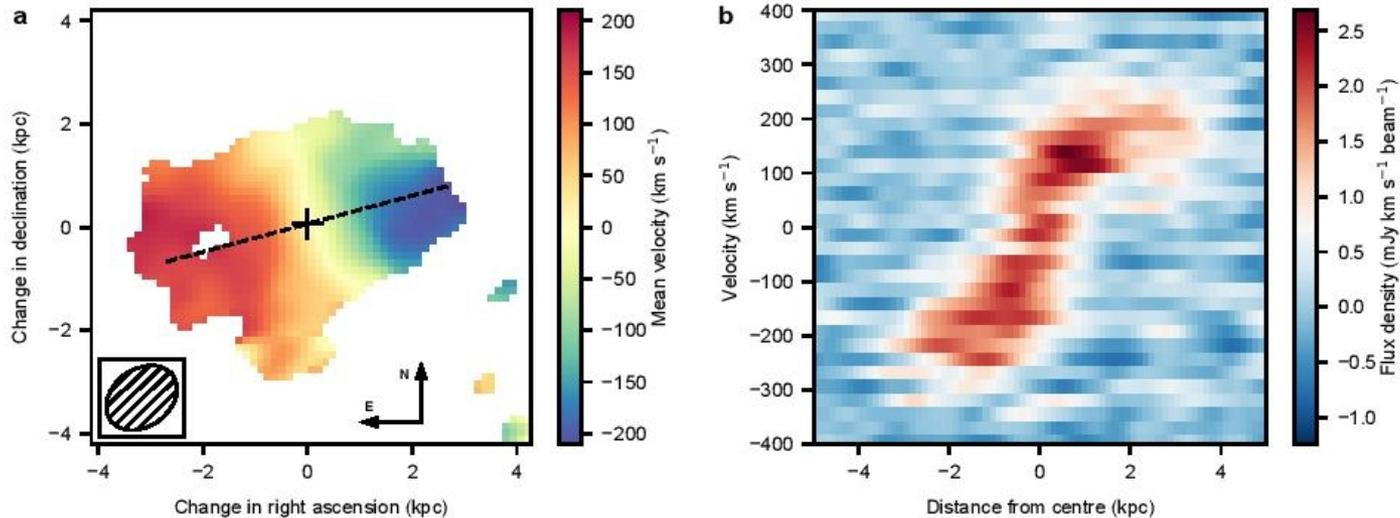
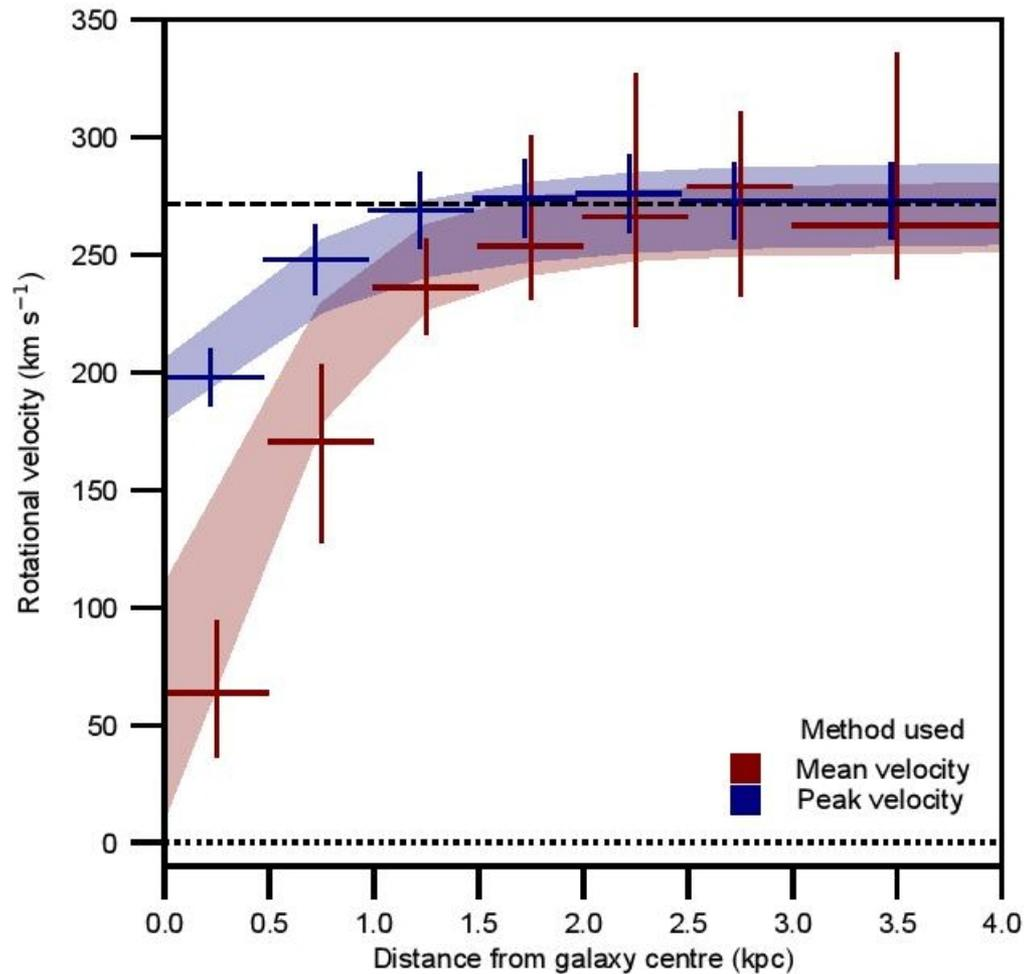


**Fig. 1. Mean velocity field and  $p$ - $v$  diagram for DLA0817g.** **a**, Mean velocity field relative to the systemic redshift of the [C II] emission ( $z = 4.2603$ ). The kinematic centre of the [C II] emission, as determined from modelling the emission (see Methods), is shown by a black plus sign. The dotted black line marks the major axis of the galaxy. The axes give relative physical (proper) distances at the redshift of the [C II] emission. The inset shows the synthesized beam of the observations. **b**, The  $p$ - $v$  diagram along the major axis of the galaxy. Distances are measured

# Кривая вращения (2 модели)

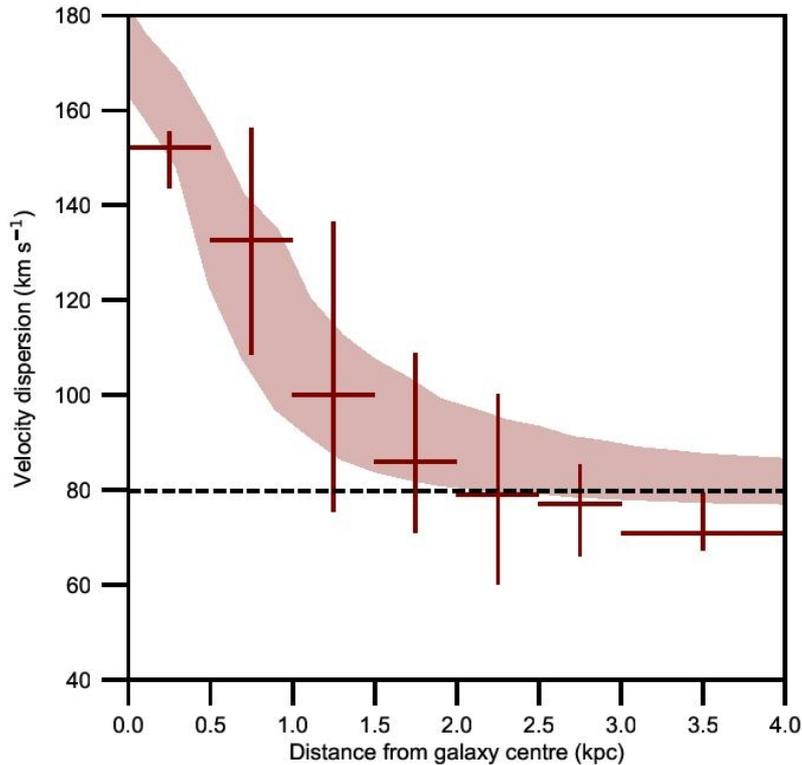


# Характеристики

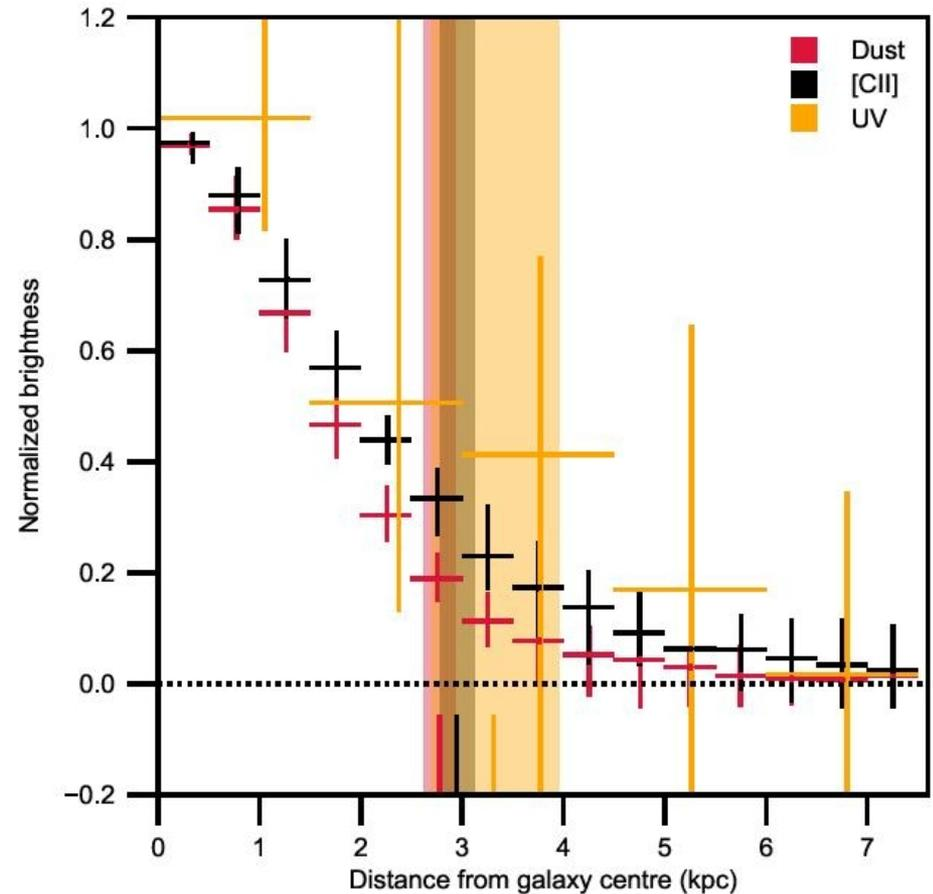
		TDconstantV	TDarctanV
R. A.	(J2000)	08:17:40.8667(4)	08:17:40.8666(4)
Decl.	(J2000)	+13:51:38.230(5)	+13:51:38.228(5)
$z$		4.26033(6)	4.26033(8)
$\alpha$	( $^{\circ}$ )	$105.2^{+1.7}_{-1.7}$	$105.7^{+1.7}_{-2.0}$
$i$	( $^{\circ}$ )	$42^{+3}_{-8}$	$42^{+4}_{-8}$
$I_0$	(mJy kpc $^{-2}$ )	$3.42^{+0.22}_{-0.22}$	$3.3^{+0.3}_{-0.7}$
$R_d$	(kpc)	$1.39^{+0.06}_{-0.05}$	$1.43^{+0.13}_{-0.08}$
$v_{\text{rot}}$	(km s $^{-1}$ )	$272^{+52}_{-13}$	$295^{+54}_{-18}$
$\sigma_v$	(km s $^{-1}$ )	$80^{+4}_{-11}$	$80^{+13}_{-11}$
$R_v$	(kpc)	—	$0.12^{+0.08}_{-0.05}$

Dust-obscured SFR, $\text{SFR}_{160\mu\text{m}}$	( $M_{\odot} \text{ yr}^{-1}$ )	$118 \pm 14$
Unobscured SFR, $\text{SFR}_{\text{NUV}}$	( $M_{\odot} \text{ yr}^{-1}$ )	$16 \pm 3$
Molecular gas mass, $M_{\text{mol}}$	( $M_{\odot}$ )	$(8.8 \pm 2.6) \times 10^{10}$
Exponential Scale length, $R_d$	(kpc)	$1.39^{+0.06}_{-0.05}$
Dynamical mass within $3R_d$ , $M_{\text{dyn}}$	( $M_{\odot}$ )	$(7.2 \pm 2.3) \times 10^{10}$
Average Toomre- $Q$ parameter, $Q$		$0.96 \pm 0.30$
$v_{\text{rot}}/\sigma_v$		$3.4^{+1.1}_{-0.3}$

# Считают, что это массивная ДИСКОВАЯ галактика



ata Fig. 5. Velocity dispersion profile for DLA0817g. The observed ve



# ArXiv: 2005.09149

A Universal fundamental plane and the  $M_{dyn} - M_{\star}$  relation for galaxies with CALIFA and MaNGA.

E. AQUINO-ORTÍZ<sup>1</sup>, S.F. SÁNCHEZ<sup>1</sup>, O. VALENZUELA<sup>1</sup>, H. HERNÁNDEZ-TOLEDO<sup>1</sup>, YUNPENG JIN<sup>2</sup>, LING ZHU<sup>3</sup>,  
GLENN VAN DE VEN<sup>4</sup>, J.K. BARRERA-BALLESTEROS<sup>1</sup>, V. AVILA-REESE<sup>1</sup>, A. RODRÍGUEZ-PUEBLA<sup>1</sup>, AND  
PATRICIA B. TISSERA<sup>5</sup>

<sup>1</sup>*Instituto de Astronomía, Universidad Nacional Autónoma de México A.P. 70-264, 04510. CDMX, México*

<sup>2</sup>*National Astronomical Observatories, Chinese Academy of Sciences, 20A Datun Road, Chaoyang District, Beijing 100101, China*

<sup>3</sup>*Shanghai Astronomical Observatory, Chinese Academy of Sciences, 80 Nandan Road, Shanghai 200030, China.*

<sup>4</sup>*Department of Astrophysics, University of Vienna, TAijrkenschanzstrasse 17, 1180 Vienna, Austria*

<sup>5</sup>*Departamento de Ciencias Físicas, Universidad Andrés Bello, 700 Fernández Concha, Las Condes, Santiago, Chile.*

(Received May, 2020; Revised Month, 2020; Accepted Month, 2020)

Submitted to ApJ

## ABSTRACT

We use the stellar kinematics for 2458 galaxies from the Mapping Nearby Galaxies at Apache point observatory (MaNGA) survey to explore dynamical scaling relations between the stellar mass  $M_{\star}$ , and the total velocity parameter at the effective radius,  $R_e$ , defined as  $S_K^2 = KV_{R_e}^2 + \sigma_{\star_e}^2$ , which combines rotation velocity  $V_{R_e}$ , and velocity dispersion  $\sigma_{\star_e}$ . We confirm that spheroidal and spiral galaxies follow the same  $M_{\star} - S_{0.5}$  scaling relation with lower scatter than the  $M_{\star} - V_{R_e}$  and  $M_{\star} - \sigma_{\star_e}$  ones. We also explore a more general two-dimensional surface known as Universal Fundamental Plane described by the equation  $\log(\Upsilon_e) = \log(S_{0.5}^2) - \log(I_e) - \log(R_e) + C.$ , which in addition to kinematics,  $S_{0.5}$ , and effective radius,  $R_e$ , it includes information of the surface brightness,  $I_e$ , and dynamical mass-to-light ratio,  $\Upsilon_e$ . We use sophisticated Schwarzschild orbit-based dynamical models for a sub-sample of 300 galaxies from the CALIFA survey to calibrate the so called Universal Fundamental Plane. That calibration allows us to propose both: (i) a parametrization to estimate the difficult-to-measure dynamical mass-to-light ratio at the effective radius of galaxies, once the internal kinematics, surface brightness and effective radius are known; and (ii) a new dynamical mass proxy consistent with

# MaNGA+SDSS-im: $v_{\text{rot}}$ , $\sigma_e$ , $L_e$ , $R_e$ , $I_e \dots$

Ballesteros et al. 2015a,b). Following this procedure our final sample for the MPL-7 comprises 2458 galaxies, of which 1653 corresponds to LTGs and 805 to ETGs. The

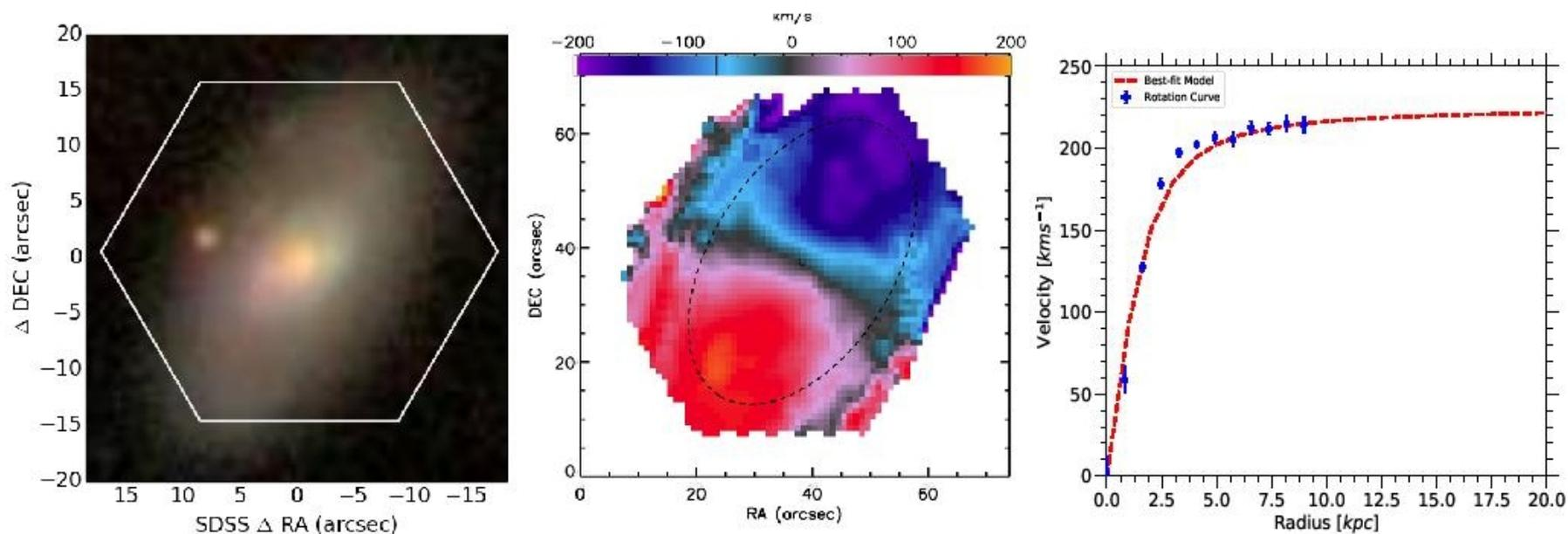


**Figure 2.** Example of spatially resolved kinematics from the MaNGA stellar kinematic maps. *Left panel:* the rgb SDSS image and the FoV covered by MaNGA for the manga-8440-12704 galaxy. *Middle panel:* the line-of-sight stellar velocity map. The dashed black ellipse represent the more external ring explored in the analysis. Only the rotation component was modeled ignoring non-circular motions. *Right panel:* the rotation curve derived from the stellar velocity map (blue symbols) with the analysis described in Section 3.4. The dashed red line represent the best-fit parametrization of Eq. (4) to the blue data points.

# Сначала была теорема вириала...

after, we define the characteristic radius,  $R$ , to be the effective radius  $R_e$ . Hence, Eq. (5) becomes:

$$A_0 V_{R_e}^2 + A_1 \sigma_{\star_e}^2 = B_0 \frac{GM_{dyn_e}}{R_e}, \quad (6)$$

with  $V_{R_e}$  as the stellar rotation velocity,  $\sigma_{\star_e}$  the stellar velocity dispersion,  $M_{dyn_e}$  the total dynamical mass enclosed at  $R_e$ ,  $G$  the gravitational constant,  $A_0, A_1$ , and  $B_0$  are correction factors obtained by fully evaluate the tensors. These correction factors could be different for each galaxy and also strong function of the formation history, dynamical state and environment of galaxies.

served data  $S_{0.5}, I_e$ , and  $R_e$  (independent variables) as follow:

$$\log(\Upsilon_e^{Sch}) = \beta_0 + \beta_1 \log(S_{0.5}) + \beta_2 \log(I_e) + \beta_3 \log(R_e), \quad (9)$$

were the  $\beta_i$  are the coefficients for each independent variable. The calibration that best recover the  $\log(\Upsilon_e^{Sch})$  yields the following values:  $\beta_0 = -0.53 \pm 0.1$ ,  $\beta_1 = 1.49 \pm 0.08$ ,  $\beta_2 = -0.72 \pm 0.03$  and  $\beta_3 = -0.63 \pm 0.05$ . We use these coefficients together with the 3 independent variables ( $S_{0.5}, I_e, R_e$ ) to calculate the fitted dynamical mass-to-light ratios,  $\log(\Upsilon_e^{fit})$ . The obligatory

2. The kinematic simplification. This means that galaxies are assumed to be isothermal spheres with isotropic velocity dispersion. Dividing the Eq. (6) by  $A_1$ , allow us to define the left-hand side as the total velocity parameter,  $S_K^2 = KV_{R_e}^2 + \sigma_{\star_e}^2$
3. The mass simplification. This means replace the total dynamical mass at the effective radius,  $M_{dyn_e}$ , with observable properties like the dynamical mass-to-light ratio within  $R_e$ ,  $\Upsilon_e$ , and the luminosity,  $L_e$ , i.e.,  $M_{dyn_e} = \Upsilon_e L_e$ . Thus, it is assumed that  $\Upsilon_e$  is constant within the considered aperture.
4. Homology, which implies that galaxies live on a plane in the  $(R_e, I_e, S_K)$  space. Thus, the correction factors  $A_0, A_1$  and  $B_0$  are very similar among galaxies.

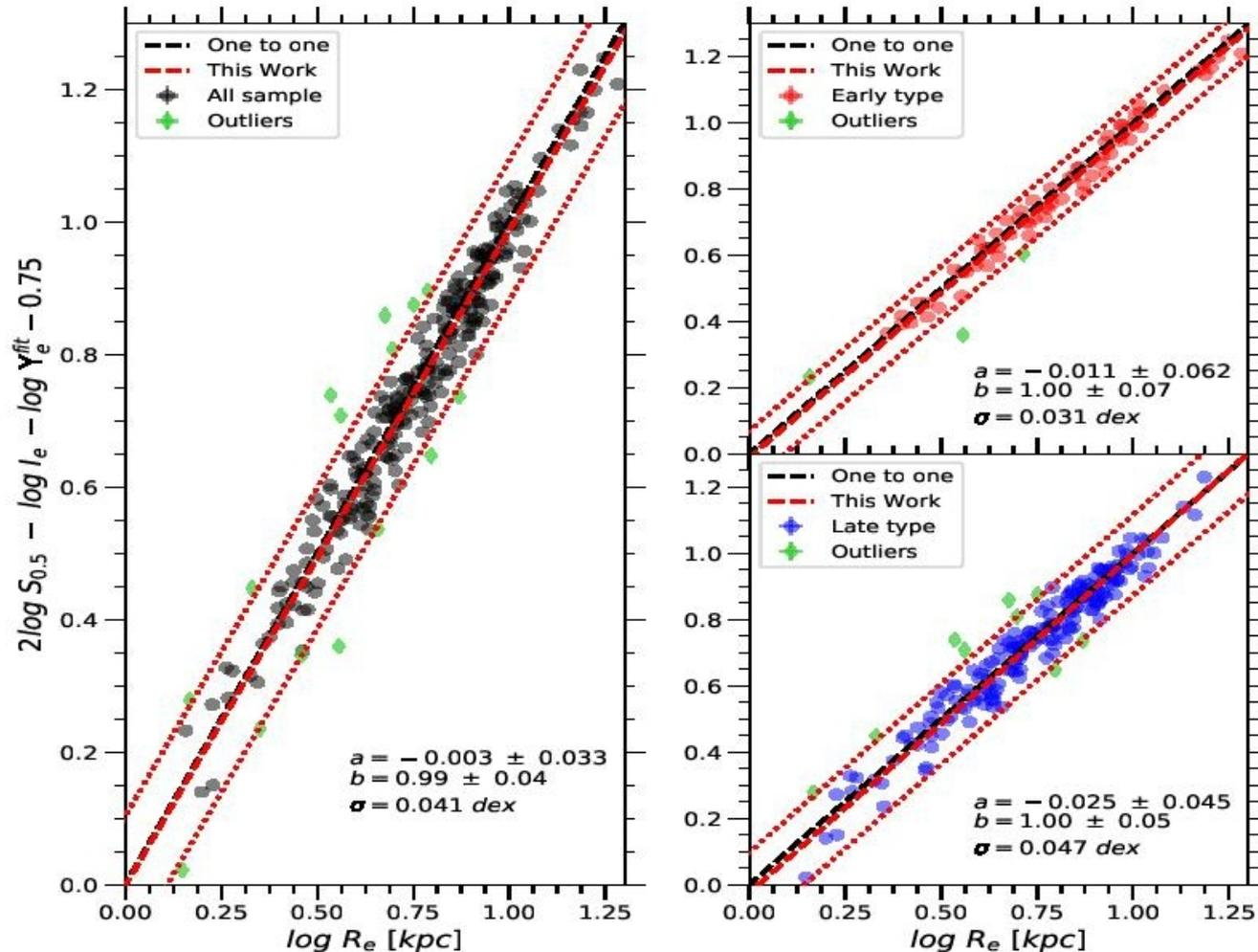
Applying the previous simplifications and assumptions we can rewrite the tensor virial theorem in terms of observational properties as follows:

$$S_K^2 = B_0 A_1' G \pi \Upsilon_e R_e I_e. \quad (7)$$

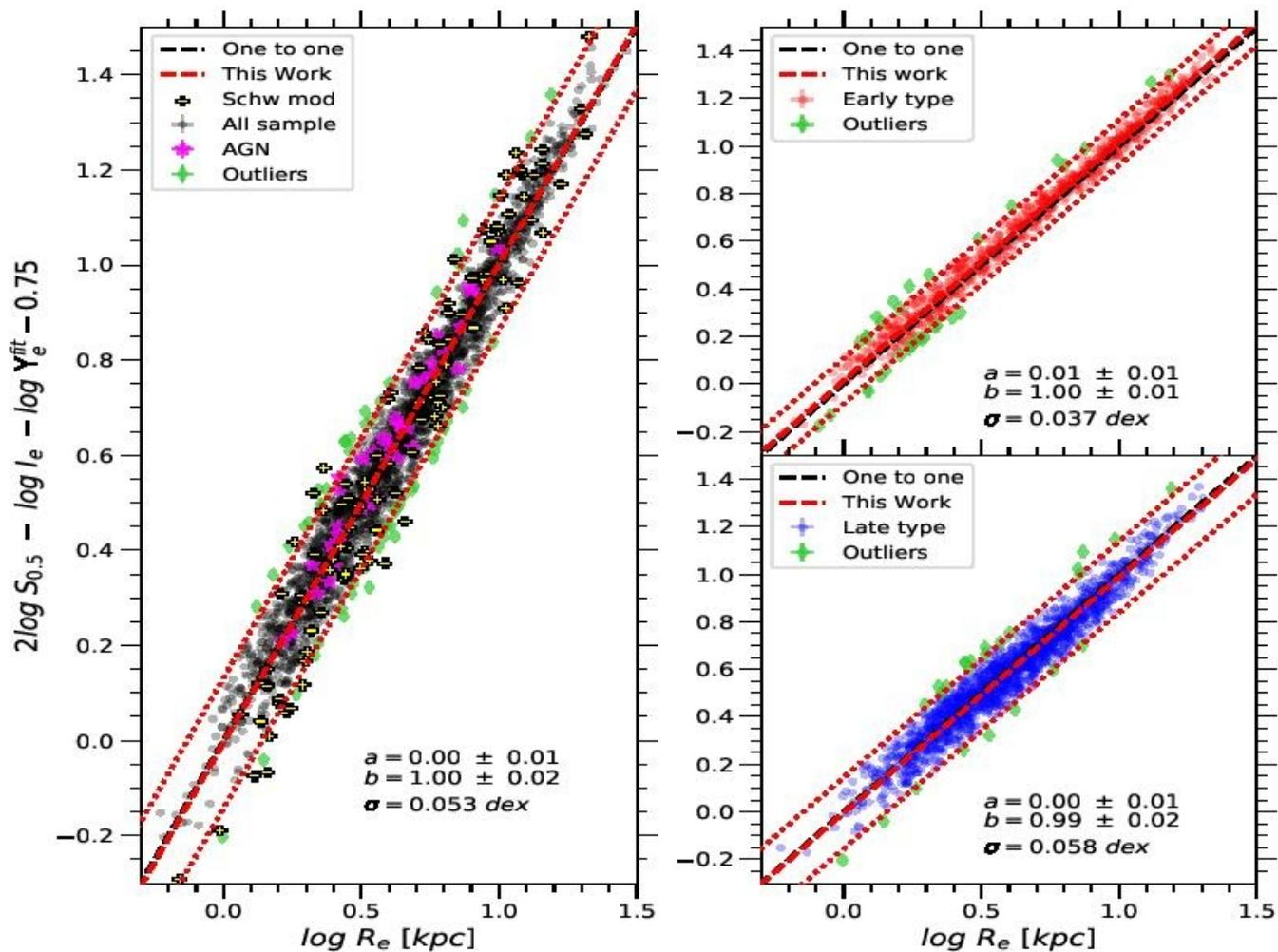
now on, we will fix  $K = 0.5$  on the total velocity parameter. Finally, we define a normalization constant  $C = G \pi B_0 A_1'$  and take the logarithm to define the Universal Fundamental Plane as follows:

$$\log(\Upsilon_e) = \log(S_{0.5}^2) - \log(I_e) - \log(R_e) + C. \quad (8)$$

# Динамические модели, чтобы откалибровать коэффициенты $\beta$ , посчитали по 300 объектам CALIFA



А вот тут отношения массы к светимости для объектов MaNGA посчитаны уже с этими коэфф.



# Ну, и сравнения звездных и динамических масс с этими M/L

